Stability of an oscillating tip in Non-Contact Atomic Force Microscopy: theoretical and numerical investigations.

Gérard Couturier, Laurent Nony, Rodolphe Boisgard, Jean-Pierre Aimé

Stability of an oscillating tip in Non-Contact Atomic Force Microscopy : theoretical and numerical investigations.

G. Couturier[1], L. Nony[2,*], R. Boisgard[1], J.-P. Aimé[1]

[1] CPMOH, UMR CNRS 5798, Université Bordeaux I

351, cours de la Libération, 33405 Talence Cedex, FRANCE

[2] L2MP, UMR CNRS 6137, Université d'Aix-Marseille III

Faculté des Sciences de Saint-Jérôme, 13397 Marseille Cedex 20, FRANCE

[*] To whom correspondence should be addressed; E-mail: laurent.nony@l2mp.fr

published in Journal of Applied Physics 91(4), pp2537-2543 (2002)

Abstract

This paper is a theoretical and a numerical investigation of the stability of a tip-cantilever system used in Non-Contact Atomic Force Microscopy (NC-AFM) when it oscillates close to a surface. No additional dissipative force is considered. The theoretical approach is based on a variationnal method exploiting a coarse grained operation that gives the temporal dependence of the nonlinear coupled equations of motion in amplitude and phase of the oscillator. Stability criterions for the resonance peak are deduced and predict a stable behavior of the oscillator in the vicinity of the resonance. The numerical approach is based on results obtained with a virtual NC-AFM developped in our group. The effect of the size of the stable domain in phase is investigated. These results are in particularly good agreement with the theoretical predictions. Also they show the influence of the phase shifter in the feedback loop and the way it can affect the damping signal.

keywords : NC-AFM, Variational principle, Stability, Virtual machine, Phase shifter, Damping variations.

I. INTRODUCTION

In recent years, the use of the Non-Contact Atomic Force Microscopy (NC-AFM) mode has shown that contrasts at the atomic scale could be achieved on semiconductors and insulators surfaces[1,2,3,4,5]. Experimental and theoretical features dedicated to the description of this dynamic mode have been widely discussed in previous papers[6,7,8,9,10,11,12]. In particular, it was shown that the high sensitivity of the oscillating tip-cantilever system (OTCS) was based on the value of the quality factor and on its nonlinear dynamics in the vicinity of the surface[10,13]. Current considerations of the authors focus on the origin of the increase of the damping signal when the tip comes close to the surface, in the range of a few angstroms. Some claim that the origin of this apparent increase could be due to the hysteretic behavior of the OTCS[10,14]. These interpretations implicitly rise the question of the stability of the OTCS when it is at the proximity of the surface.

The aim of this paper is to show from a theoretical and a numerical point of view that the nonlinear dynamics of the OTCS leads to various stability domains of its resonance peak that may help to understand the reason why the NC-AFM mode, while being so sensitive, keeps, in most of cases, a stable behavior. In other words, this work is an attempt to show that, if no additional dissipative force is considered between the tip and the surface, an apparent increase of the damping signal cannot be the consequence of the nonlinear behavior of the OTCS.

The paper is organized as follow. The first part is dedicated to a description of the nonlinear behavior of the OTCS at the proximity of the surface. To do so, a specific theoretical frame based on a variational method using a coarse grained operation has been developed. This gives the explicit temporal dependance of the OTCS equations of motion. These equations are the basis to analyze the stability of the stationary state. A large part of this work is detailed in ref.[15]. Experimentally, as the NC-AFM mode requires the use of a feedback loop to maintain constant the amplitude at the resonance frequency, which in turn requires to maintain constant the phase of the oscillator around its resonance value, e.g. $-\pi/2$ rd, the phase variations of the OTCS will be extracted and discussed. The second part of the paper deals with numerical results obtained with the virtual NC-AFM[16] which is very similar to the experimental machine. These results show unambiguously the contribution of the phase shifter in the feedback loop and the way it can lead to damping variations.

II. THEORETICAL APPROACH OF THE NC-AFM

The present section is divided into three parts. The first one details the specific theoretical frame for the obtention of the equations of motion in amplitude and phase of the OTCS. A coarse-grained method gives the equation describing the time evolution of the stationary state of the OTCS as a function of the coupling term between the tip and the surface. The second part is a description of the distortion of the resonance peak as a function of the distance. This part was detailed in ref.[15] so that only the main results are given. The results provide the basis of the discussion about the stability of the branches which is detailed in the third part.

A. Theoretical frame

We search a solution to the temporal evolution of the OTCS by using a variational solution based on the principle of least action. Even though this approach exploits the same physical concepts than the one which had led to the coupled equations in amplitude and phase of the stationary state of the OTCS[10,17], it appears to be more general since here, the temporal dependance is explicitly obtained. We start from the definition of the action of the OTCS coupled to an interaction potential :

$$S = \int_{t_a}^{t_b} \mathcal{L}\left(z, \dot{z}, t\right) dt, \tag{1}$$

where $\mathcal{L}$ is the Lagrangian of the system and $z\left(t\right)$ the position of the tip with time[17] :

$$\begin{aligned} \mathcal{L}\left(z, \dot{z}, t\right) &= \mathcal{T} - \mathcal{V} + \mathcal{W} \\ &= \frac{1}{2} m^* \dot{z}\left(t\right)^2 - \left[\frac{1}{2} k_c z\left(t\right)^2 - z\left(t\right) \mathcal{F}_{exc} \cos\left(\omega t\right) + V_{int}\left[z\left(t\right)\right]\right] - \frac{m^* \omega_0}{Q} z(t) \underline{\dot{z}}\left(t\right) \end{aligned} \tag{2}$$

ω_0, Q, m^* and $k_c = m^* \omega_0^2$ are respectively the resonance pulsation, quality factor, effective mass and cantilever' stiffness of the OTCS. $\mathcal{F}_{exc}$ and ω are the external drive force and drive pulsation. Due to the large quality factor, we assume that a typical temporal solution is on the form :

$$z\left(t\right) = A\left(t\right) \cos\left[\omega t + \varphi\left(t\right)\right], \tag{3}$$

where $A(t)$ and $\varphi(t)$ are assumed to be slowly varying functions with time compared to the period $T = 2\pi/\omega$. The underlined variables of $\dot{\underline{z}}(t)$ in equ.2, e.g. $\underline{A}(t)$, $\underline{\varphi}(t)$, $\dot{\underline{A}}(t)$ and $\underline{\dot{\varphi}}(t)$, are calculated along the physical path, thus they are not varied into the calculations[18].

To describe the interaction between the tip and the surface, the attractive coupling force is assumed to derive from a sphere-plane interaction involving the disperse part of the Van der Waals potential[19] :

$$V_{int}[z(t)] = -\frac{HR}{6[D - z(t)]} \tag{4}$$

H, R and D are the Hamaker constant, the tip's apex radius and the distance between the surface and the equilibrium position of the OTCS.

The equations of motion in amplitude and phase of the OTCS are obtained by considering the following coarse-grained operation. Let's assume a long duration $\Delta t = t_b - t_a$ with $\Delta t \gg T$ and calculate the action as a sum of small pieces of duration T :

$$S = \sum_n \int_{nT}^{(n+1)T} \mathcal{L}(z, \dot{z}, t)\, dt = \sum_n \left(\frac{1}{T} \int_{nT}^{(n+1)T} \mathcal{L}(z, \dot{z}, t)\, dt \right) T = \sum_n \mathcal{L}_e T \tag{5}$$

$\mathcal{L}_e$ is the mean Lagrangian during one period and appears as an effective Lagrangian for a large time scale compared to the period. Owing to the quasi-stationary behavior of the amplitude and the phase over the period, the effective Lagrangian is calculated by keeping them constant during the integration. The calculations give :

$$\begin{aligned} \mathcal{L}_e\left(A, \dot{A}, \varphi, \dot{\varphi}\right) \;=\; & \frac{m^*}{4}\left[\dot{A}^2 + A^2\left(\omega + \dot{\varphi}^2\right)\right] - \frac{k_c A^2}{4} + \frac{\mathcal{F}_{exc} A \cos(\varphi)}{2} - \frac{1}{T}\int_0^T V_{int}[z(t)]\, dt \\ & - \frac{m^* \omega_0}{2Q}\left[A\underline{\dot{A}}\cos\left(\varphi - \underline{\varphi}\right) - A\underline{A}\left(\omega + \underline{\dot{\varphi}}\right)\sin\left(\underline{\varphi} - \varphi\right)\right] \end{aligned} \tag{6}$$

Note that the effective Lagrangian is now a function of the new generalized coordinates A, φ and their associated generalized velocities $\dot{A}$, $\dot{\varphi}$. At this point, remembering that the period is small regardless to $\Delta t = t_b - t_a$ during which the total action is evaluated, the continuous expression of the action is :

$$S = \int_{t_a}^{t_b} \mathcal{L}_e\left(A, \dot{A}, \varphi, \dot{\varphi}\right) d\tau, \tag{7}$$

where the measure $d\tau$ is such that $T \ll d\tau \ll \Delta t$.

Applying the principle of least action $\delta S = 0$ to the functional $\mathcal{L}_e$, we obtain the Euler-Lagrange equations for the effective Lagrangian. Thus, the amplitude and phase equations

of motion of the OTCS coupled to the surface through an interaction involving the disperse part of the Van der Waals potential are obtained :

$$\begin{cases} \ddot{a} = \left[(u+\dot{\varphi})^2 - 1\right] a - \dfrac{\dot{a}}{Q} + \dfrac{\cos(\varphi)}{Q} + \dfrac{a\kappa_a}{3\left(d^2-a^2\right)^{3/2}} \\ \ddot{\varphi} = -\left(\dfrac{2\dot{a}}{a} + \dfrac{1}{Q}\right)(u+\dot{\varphi}) - \dfrac{\sin(\varphi)}{aQ} \end{cases} , \tag{8}$$

In equ.8, specific notations were used. $d = D/A_0$ is the reduced distance between the location of the surface and the equilibrium position of the OTCS normalized to the resonance amplitude $A_0 = Q\mathcal{F}_{exc}/k_c$, $a = A/A_0$ is the reduced amplitude, $u = \omega/\omega_0$ is the reduced drive frequency normalized to the resonance frequency of the free OTCS and $\kappa_a = HR/\left(k_c A_0^3\right)$ is the dimensionless parameter that characterizes the strength of the interaction.

B. Resonance frequency shift

The equations of motion of the stationary solutions a and φ are obtained by setting $\dot{a} = \dot{\varphi} = 0$ and $\ddot{a} = \ddot{\varphi} = 0$ in equ.8 and lead to two coupled equations of the sine and cosine of the phase of the OTCS previously calculated[17] :

$$\begin{cases} \cos(\varphi) = Qa(1-u^2) - \dfrac{aQ\kappa_a}{3\left(d^2-a^2\right)^{3/2}} \\ \sin(\varphi) = -ua \end{cases} , \tag{9}$$

Solving equ.9 gives the relationship between the frequency and the amplitude at a given distance d[10] :

$$u_{\pm}(a) = \sqrt{\frac{1}{a^2} - \frac{1}{4Q^2}\left(1 \mp \sqrt{1 - 4Q^2\left(1 - \frac{1}{a^2} - \frac{\kappa_a}{3\left(d^2-a^2\right)^{3/2}}\right)}\right)^2} \tag{10}$$

The signs plus and minus are deduced from the sign of $\cos(\varphi)$ and correspond to values of the phase ranging from 0 to $-90°$ (u_-, $\cos(\varphi) > 0$) or from $-90°$ to $-180°$ (u_+, $\cos(\varphi) < 0$), in agreement with the sign convention of the phase in equ.3. From equ.10 is calculated the resonance peak at any reduced distance for a given strength of the sphere-surface interaction and equ.9 give the associated phase variations. The two branches define the distortion of the resonance peak as a function of d. u_- gives the evolution of the resonance peak for frequency values below the resonance one and u_+ for frequency values above the resonance.

In fig.1 is given the distortion of the resonance peak vs. the reduced distance d. For large values of d, e.g. when the surface is far from the OTCS, the nonlinear effects are negligible and the peak keeps a well-defined Lorentzian shape (see equ.10 with $\kappa_a = 0$). When the OTCS is approached towards the surface, because the interaction is attractive, the resonance peak starts to distort towards the low frequencies. The distortion of the peak increases as d decreases. On the fig.1, the branches that are supposed unstable are shown with dashed lines.

Using equ.10, the resonance frequency shift as a function of the distance d is obtained by setting $a = 1$. This former condition ensures the required condition for the NC-AFM mode. Thus, the normalized frequency shift, $(\nu - \nu_0)/\nu_0$, is given by $u - 1$[10] :

$$u_{\pm}(d) - 1 = \sqrt{1 - \frac{1}{4Q^2}\left(1 \mp \sqrt{1 + \frac{4}{3}\frac{Q^2\kappa_a}{(d^2-1)^{3/2}}}\right)^2} - 1 \tag{11}$$

The frequency shift given by equ.11 vs. d can be deduced from the fig.1 (see the arrows on the figure). Following the previous discussion about the stability of the different parts of the resonance peak during the distortion, since the measure is performed as a function of d with $a = 1$, no bistable behavior can be observed.

However, in the vicinity of the resonance the branches u_+ and u_- become very close (see for instance fig.1 with $d_3 = 1.012$). Therefore, even with an oscillation amplitude kept constant, question rises about the ability of the OTCS to remain on the same branch. Qualitatively, one may expect that around $a \cong 1$, the branch u_- is unstable and u_+ is stable (see fig.1). If this is true, any small fluctuation of the oscillation amplitude might produce a jump from one branch to the other one as discussed in refs.[10,14]. Since the branch u_- seems to be unstable, a jump to this branch should lead to an abrupt decrease of the amplitude, which in turn might produce an apparent abrupt increase of the damping signal as a consequence of the hysteretic behavior. Because such a jump is, in most of cases, never observed, it becomes useful to determine more accurately the stability of the two branches.

C. Stability criterions

The stability of the branches $u_\pm$ of the resonance peak is obtained from equations of motion of the OTCS (see equ.8). By linearizing these equations around the stationary solution

(now identified by the index "s") and using classical considerations of the linear theory, one gets the stability criterions of the branches $u_\pm$. The stability criterions can be expressed from the derivatives $da_s/du_\pm$ of the branches and reduced to the simple expression[15]:

$$\begin{cases} \dfrac{da_s}{du} > 0 \qquad \text{and} \qquad \cos(\varphi_s) > a_s/(2Q) \qquad (i) \\ \qquad\qquad\qquad\qquad \text{or} \\ \dfrac{da_s}{du} < 0 \qquad \text{and} \qquad \cos(\varphi_s) < a_s/(2Q) \qquad (ii) \end{cases} \tag{12}$$

The figs.2*(a)* and *(b)* show the distortion of the resonance peak and of the associated phase curve, respectively. The figs.3*(a)* and 3*(b)* are zooms on the region α of the figs.2*(a)* and *(b)*, respectively.

For the branch u_+, da_s/du_+ being always negative and the associated value of the phase being always defined beyond $-\pi/2$ (see section II B), the criterion (ii) implies that u_+ is always stable, whatever the value of a_s.

For u_-, the sign of the derivative changes twice. For this branch, the phase is always defined above $-\pi/2$. Therefore on the lower part of the branch (small a), $da_s/du_- > 0$ and the criterion (i) indicates that the branch is locally stable. When da_s/du_- becomes negative (see fig.2*(a)*), because $\varphi_s > -\pi/2$ (see fig.2*(b)*), the criterion (i) is no more filled. As a consequence, u_- is locally unstable and the instability is precisely located where the infinite tangent appears. On the upper part of the resonance peak, the curvature of u_- changes again and $da_s/du_- > 0$ (see fig.3*(a)*), implying that it is again a locally stable domain. Thus the branches u_- and φ_- exhibit two stable domains and one unstable.

Note also that the resonance condition is deduced from $da_s/du = 0$ which implies $\cos(\varphi_s) = a_s/(2Q)$, or equivalently $u_- = u_+$ or again $\varphi_- = \varphi+$. This equality is the usual resonance condition of a free harmonic oscillator. If $a_s = 1$, e.g. without any coupling, the resonance phase is therefore $\varphi_s = \arccos[1/(2Q)]$. For the OTCS we used, $Q \simeq 500$, and so $\varphi_s \cong -\pi/2$. But taking into account the fact that the coupling only slightly modifies the value of the resonance amplitude, $a_s \simeq 1.0013$ (see fig.2*(a)*), we still obtain $\varphi_s \cong -\pi/2$ so that we can consider that the nonlinear resonance is always given by the relationship $\varphi_s = -\pi/2$.

Therefore the theoretical approach foresees that u_+ is always stable but that also a small domain of u_- around the resonance value remains stable. If the resonance value would have

been located at the point where da_s/du_- is infinite, an infinitely small fluctuation would have been able to generate an abrupt increase of the damping signal as discussed previously and suggested in ref.[10], or more recently in ref.[14]. Experimentally, an electronic feedback loop keeps constant the amplitude of the OTCS so that its phase is located around $-\pi/2$ (see section below). As a consequence, question rises about the size of the stable domain in phase around $-\pi/2$. If any fluctuation around $-\pi/2$ makes the phase going beyond the stable domain, the OTCS behavior becomes unstable. For $Q = 500$, the size of the stable domain is of about $2.6.10^{-2}$ rd (see fig.3*(b)*) whereas it's reduced to $2.6.10^{-3}$ rd for $Q = 5000$ (data not shown). Thus, if the electronic loop is able to control the phase locking with a better accuracy than $2.6.10^{-3}$ rd, the OTCS will be locked on a stable domain.

Therefore, if the setpoint of the oscillator is properly located at the $-\pi/2$ value throughout an experiment, this value corresponds to a stable domain and consequently will neither give rise to amplitude or phase variations nor to damping variations.

III. VIRTUAL NC-AFM RESULTS

In a recent paper, we have described a virtual NC-AFM machine built using the *Matlab* language and the *Simulink* toolbox[16]. This machine is very similar to our own experimental hybrid machine built with *Digital Instruments*[20] and *Omicron*[21] blocks. The virtual machine has been extensively used to study the frequency shift and the damping signal in the approach-retract mode. Two types of situations have been investigated : $i-$ the first one corresponds to the case where no dissipative force is introduced in the tip-surface interaction, $ii-$ the second one deals with dissipative forces. In both cases an attractive sphere-plane Van der Waals interaction is taken into account.

In spite of previous results that have already shown that the damping signal could be considered as a constant when no dissipative force was introduced[16], here we want to investigate with the virtual machine the stability of the OTCS by looking accurately at its phase variations within the electronic feedback loop that maintains constant the amplitude of the oscillations and compare these results with the theoretical predictions. To do so, we still do not consider any additional dissipative force.

The theoretical results have led to the conclusion that, provided that the OTCS phase is in the close vicinity of $-\pi/2$, this setpoint corresponds to a stable branch. As a consequence,

the questions are : $i-$ What is the part of the feedback loop that controls the size of the phase stable domain of the OTCS around -$\pi/2$ rd ? and $ii-$ Would it be possible to change the parameters of this element in order to change the size of the phase stable domain and thus observe phase variations? As a consequence of these changes, variations of the damping signal should also be observed.

A. The phase shifter of the feedback loop

In fig.4 is drawn a very simplified schematic diagram of the feedback loop of the NC-AFM (for more details, see ref.[16]). Usually, the phase $\phi(\omega)$ of the phase shifter transfer function is adjusted to $-3\pi/2$ so that the loop oscillates at ν_0 which is the free resonance frequency of the cantilever, corresponding to a tip-surface distance $D \to \infty$. We recall that the oscillations of the loop are ruled by the relation :

$$\phi(\omega) + \varphi(\omega) = 0 \pm 2n\pi, \tag{13}$$

where n is an integer and $\varphi(\omega)$ is the phase difference between the oscillations and the excitation of the cantilever. If the setpoint is fixed to the resonance frequency, then $\varphi(\omega_0) = -\pi/2$. The phase adjustment in the *Omicron* electronics is obtained by changing the bias of varicap diodes[22]. The phase shifter transfer function in terms of the p Laplace variable can be written as $H(p) = \left(\frac{1-\tau p}{1+\tau p}\right)^2$, the time constant τ being adjusted by the user such that, at the resonance :

$$\phi(\omega_0) = -4\arctan(\tau\omega_0) = -\frac{3\pi}{2} \tag{14}$$

When the tip-surface distance D is reduced, due to the coupling, ω_0 decreases. As a consequence, $\phi(\omega_0)$ and $\varphi(\omega_0)$ and are no more equal to $-3\pi/2$ and $-\pi/2$ respectively. According to equ.13, the variation of $\varphi(\omega)$ is governed by the one of $\phi(\omega)$. Assuming a small variation around the resonance frequency $\Delta\omega = \omega - \omega_0$, one gets :

$$\phi(\omega) \simeq -3\pi/2 - \frac{4\tau}{1+(\tau\omega_0)^2}\Delta\omega \tag{15}$$

As D decreases, $\Delta\omega$ is negative. Therefore $\phi(\omega)$ becomes larger than $-3\pi/2$ and $\varphi(\omega)$ smaller than $-\pi/2$. The decrease of $\varphi(\omega)$, $\varphi(\omega) \lesssim -\pi/2$, means that the phase of the

OTCS follows the phase branch associated to u_+, φ_+, which is always stable (see fig.2*(b)*). Thus the loop is always stable. Moreover, the hypothesis implying that $\varphi(\omega)$ keeps a value close to $-\pi/2$ is a very good assumption. To proof that, let us consider for instance $\nu_0 = 150$ kHz, which is a reasonable value for a cantilever. Therefore $\tau = 2.56.10^{-6}$ s (see equ.14). Assuming now a large frequency shift, $\Delta\nu = -200$ Hz, we get $\Delta\phi(\omega) = 1.9.10^{-3}$ rd and therefore $\Delta\varphi(\omega) = -1.9.10^{-3}$ rd. In spite of the rough assumption of a first order expansion of the phase of the phase shifter, the typical phase variations of the OTCS around the nonlinear resonance are less than 2.10^{-3} rd. This implies that the machine properly follows the nonlinear resonance, even when large frequency shifts are considered.

The curves [a] in figs.5 and 6 show the phase $\varphi(\omega)$ and the damping signal vs. the distance D, respectively. As expected, the variations are very weak.

B. "Controlled" damping variations

If we want to observe the phase instability predicted by the theoretical calculations, the phase shifter transfer function should have been on the form $d\phi(\omega)/d\omega > 0$ around ω_0. A possible expression of such a transfer function would be : $H(p) = \left(\frac{1+\tau p}{1-\tau p}\right)^2$. Experimentally, this form is not feasible and even if it were, the loop would become unstable and therefore no stationary state could be reached. The reason is that the inverse Laplace transform of $1/(1-\tau p)$ varies as $e^{t/\tau}$ which diverges as $t \to \infty$.

In the virtual machine, it is possible to implement a phase shifter with a slope $d\phi(\omega)/d\omega$ larger than the phase shifter built by *Omicron*. We have retained the following transfer function which is easy to do with electronic components :

$$H(p) = \left(\frac{p^2 - \frac{\omega_1}{Q_1}p + \omega_1^2}{p^2 + \frac{\omega_1}{Q_1}p + \omega_1^2}\right) \tag{16}$$

The parameters ω_1 and Q_1 may be adjusted to obtain for instance $\phi(\omega_0) = -3\pi/2$. The phase of the transfer function is then :

$$\phi(\omega) = -2\arctan\left(\frac{\omega_1\omega}{Q_1(\omega_1^2 - \omega^2)}\right) \tag{17}$$

For a small frequency shift, $d\phi(\omega)/d\omega \simeq -4Q_1/\omega_0$. Keeping the same values than previously $\nu_0 = 150$ kHz and $\Delta\nu = -200$ Hz and assuming $Q_1 = 50$, we now obtain a change $\Delta\phi(\omega)$ of about 0.26 rd. Consequently, the change $\Delta\varphi(\omega)$ becomes larger (see the curve [b] in fig.5) and we now observe an increase of the damping signal as shown in fig.6, curve [b].

The previous examples are pedagogical cases for which an arbitrary large value of the slope of the phase of the phase shifter was considered. The ideal phase shifter should maintain the phase $\phi(\omega_0)$ at $-3\pi/2$ so that the frequency of the loop remains equal to the resonance frequency of the cantilever. This is not possible in practice, however it is clear that the solution retained by *Omicron* is very close to the ideal case $\phi(\omega_0) = -3\pi/2$ because $d\phi(\omega)/d\omega$ is very weak.

IV. CONCLUSION

A variational method based on a coarse-grained operation has been used to investigate in details the stability of an oscillating tip-cantilever system near a surface. The tip-surface interaction is described by Van der Waals forces. Results show that the resonance peak of the oscillator can be described from two branches. The first one, named u_+, corresponds to frequencies larger than the resonance. Stability criterions deduced foresee that it is always stable. The second one, u_-, may be decomposed into three domains : two are stable and one is unstable. The second stable domain of u_- is small and is defined at the upper extremity of the resonance peak. The phase at the resonance $\varphi(\omega_0) = -\pi/2$ is at the overlap of the u_+ and of this former second stable domain of u_-, thus the setpoint $\varphi(\omega_0) = -\pi/2$ belongs to a stable zone.

This result is of great importance to understand the stability in NC-AFM. In this technique, the phase of the cantilever is adjusted to $-\pi/2$ within an electronic feedback loop as the tip-surface distance D is infinite. In the approach mode, the frequency of the loop decreases, consequently the phase becomes smaller than $-\pi/2$ because the slope $d\phi(\omega)/d\omega$ of the phase of the phase shifter transfer function is always negative. Thus the oscillator always "slides" along u_+ and the system is unconditionally stable. This is what is usually observed experimentally and confirmed by the results of the virtual NC-AFM we have built. Because the slope $d\phi(\omega)/d\omega$ and the frequency shift are very weak, we may consider that the phase $\varphi(\omega_0)$ of the oscillator is always very close to $-\pi/2$, typical variations being less

than 2.10^{-3} rd. Consequently, the damping signal keeps constant if no dissipative force is introduced in the tip-surface interaction.

Referencecs

[1] Geissibl, F.J. *Science* **267**, 68–71 (1995).

[2] Sugarawa, Y., Otha, M., Ueyama, H., Morita, S. *Science* **270**, 1646–1648 (1995).

[3] Kitamura, S., Iwatsuki, M. *Jpn. J. Appl. Phys.* **35**, L668–L671 (1996).

[4] Bammerlin, M., Lüthi, R., Meyer, E., Baratoff, A., Lü, J., Guggisberg, M., Gerber, C., Howald, L., Güntherodt, H.J. *Probe Microscopy* **1**, 3–9 (1996).

[5] Schwarz, A., Allers, W., Schwarz, U.D., Wiesendanger, R. *Appl. Surf. Sci.* **140**, 293–297 (1999).

[6] Albrecht, T.R., Grütter, P., Horne, D., Rugar, D. *J. Appl. Phys.* **69**(2), 668–673 (1991).

[7] Anczycowsky, B., Krüger, D., Fuchs, H. *Phys. Rev. B* **53**(23), 15485–15488 (1996).

[8] Geissibl, F.J. *Phys. Rev. B* **56**(24), 16010–16015 (1997).

[9] Wang, L. *Appl. Phys. Lett.* **73**(25), 3781–3783 (1998).

[10] Aimé, J.-P., Boisgard, R., Nony, L., Couturier, G. *Phys. Rev. Lett.* **82**(17), 3388–3391 (1999).

[11] Sasaki, N., Tsukada, M. *App. Surf. Sci.* **140**(3-4), 339–343 (1999).

[12] Dürig, U. *Surf. Interface Anal.* **27**, 462 (1999).

[13] Aimé, J.-P., Couturier, G., Boisgard, R., Nony, L. *Appl. Surf. Sci.* **140**, 333–338 (1999).

[14] Gauthier, M., Tsukada, M. *Phys. Rev. Let.* **85**(25), 5348–5351 (2000).

[15] Nony, L., Boisgard, R., Aimé, J.-P. Accepted in the European Physical Journal B.

[16] Couturier, G., Aimé, J.-P., Salardenne, J., Boisgard, R. to be published in European Physical Journal Applied Physics, (2001).

[17] Nony, L., Boisgard, R., Aimé, J.-P. *J. Chem. Phys.* **111**(4), 1615–1627 (1999).

[18] Goldstein, H. *Classical Mechanics.* Addison-Wesley, Reading, (1980).

[19] Israelachvili, J.N. *Intermolecular and Surface Forces.* Academic Press, New York, 2nd edition, (1992).

[20] Digital Instruments, Veeco Metrology Group, Santa Barabara CA (USA).

[21] Omicron, Vacuumphysik, GmbH.

[22] Omicron. *SCALA Electronics Technical Reference Manual.*, (1997). Version 1.

Figures

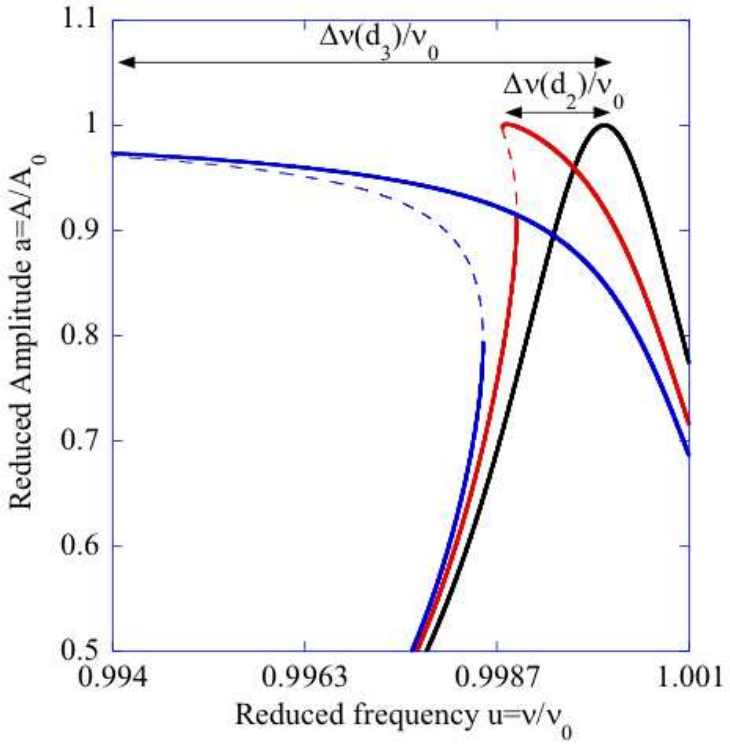

FIG. 1: Distortion of the resonance peak computed from equ.10 for three values of the distance, $d_1 = 2$, $d_2 = 1.11$ and $d_3 = 1.012$. The numerical parameters are $A_0 = 20nm$, $Q = 400$ and $\kappa_a = 8.10^{-4}$. For an attractive coupling, the peak is more and more distorted towards the low frequencies as d is reduced, e.g. the surface is approached. For each value of d, the unstable domains of u_- are shown with dashed lines. The arrows indicate the resonance frequency shift vs. d.

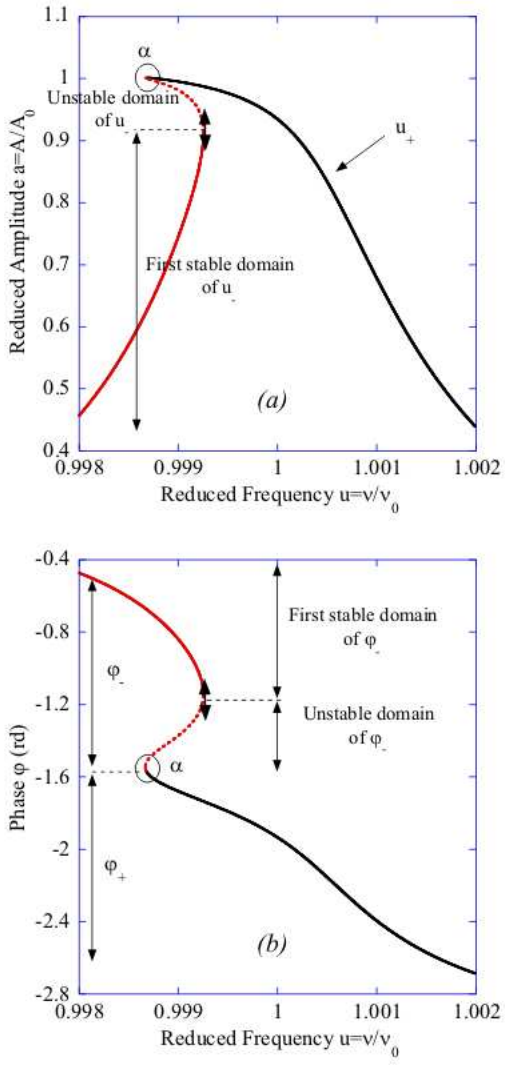

FIG. 2: *(a)*- Distortion of the resonance peak computed from equ.10. The numerical parameters are $d = 1.05$, $A_0 = 10nm$, $Q = 500$ and $\kappa_a = 2.5.10^{-4}$. The stability criterions foresee that u_+ is always stable whereas u_- exhibits two stable domains (continuous lines) and one unstable (dashed lines). The domains are separated by the spots where the derivative da/du_- is infinite. *(b)*- Distortion of the phase curve computed from equs.9 associated to the resonance peak. As a consequence of the stability of u_+, φ_+ is always stable whereas φ_- exhibits two stable domains and one unstable.

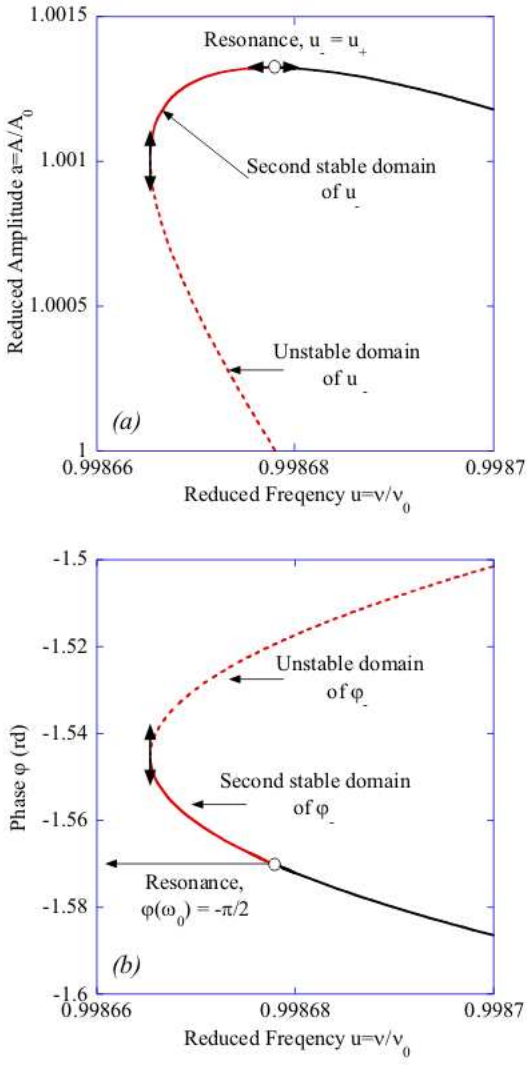

FIG. 3: *(a)*- Zoom in the region α of the resonance peak. As da/du_- becomes infinite again, the criterions define a new domain of u_- which is stable. The resonance is located where $u_+ = u_-$. *(b)*- Zoom in the region α of the phase curve. The resonance is located at $-\pi/2$ where $\varphi_+ = \varphi_-$ and belongs to a stable domain.

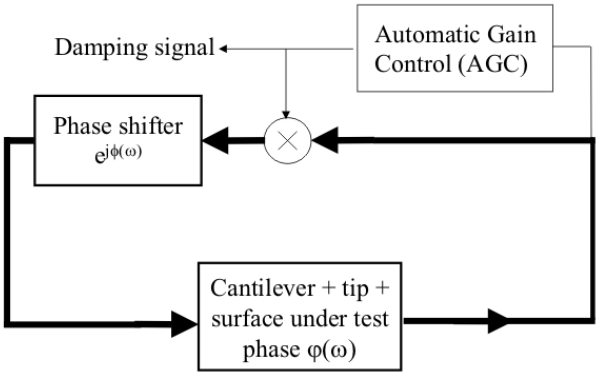

FIG. 4: Schematic diagram of the feedback loop used in the virtual NC-AFM which is very similar to the one of the experimental machine.

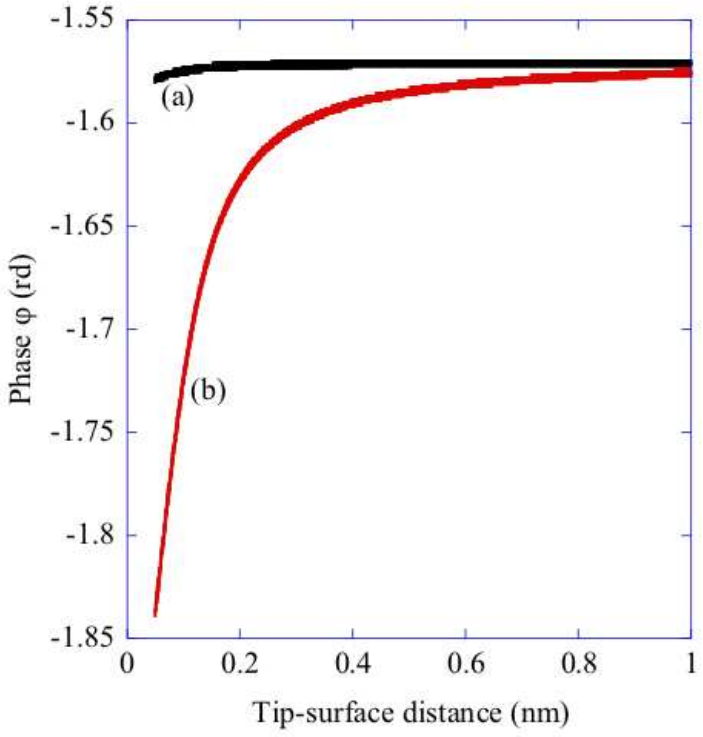

FIG. 5: Variations of the phase of the OTCS $\varphi(\omega)$ within the feedback loop vs. the distance D computed from the virtual NC-AFM. The numerical parameters are : resonance amplitude $A_0 = 15$ nm, spring constant $k_c = 40$ N.m^{-1}, quality factor $Q = 5000$, tip's radius $R = 10$ nm and Hamaker constant $H = 2.10^{-19}$ J. Curve [a] : The phase $\phi(\omega)$ of the transfer function $H(p)$ of the phase shifter is the one given by equ.14, e.g. is similar to the experimental machine. As D decreases, $\varphi(\omega)$ becomes weakly smaller than $-\pi/2$ (less than 2.10^{-3} rd), therefore follows the stable branch φ_+. The machine follows accurately the setpoint, which is always stable, even when the tip is in the very close vicinity of the surface. The associated damping variation nearly no varies (see fig.6). Curve [b] : $\phi(\omega)$ is the phase of $H(p)$ whose expression is given by equ.16. Around $-\pi/2$, the slope $d\phi(\omega)/d\omega$ is larger than in case [a] so that $\varphi(\omega)$ decreases more quickly. As a consequence, the damping signal increases.

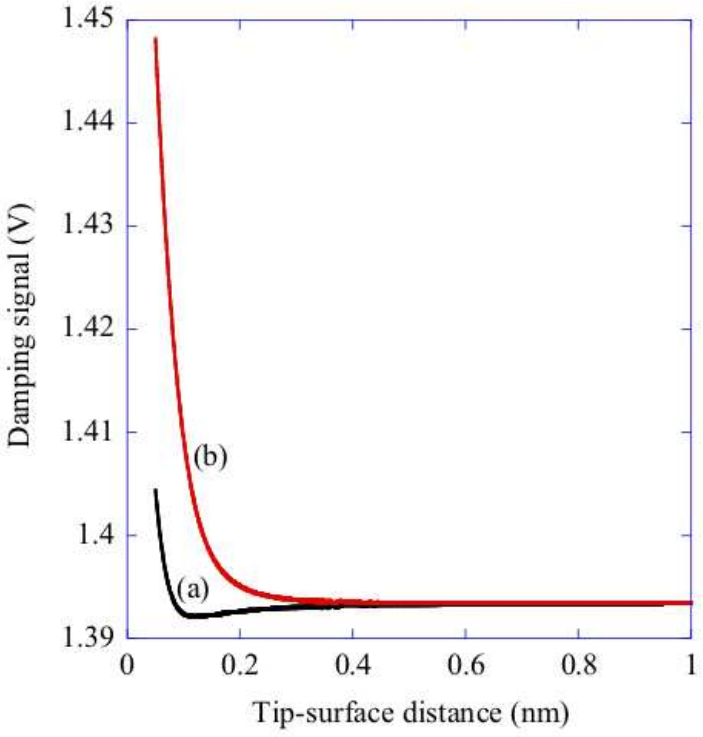

FIG. 6: Variations of the damping signal vs. the distance D. Curve [a] : No damping variation is observed if the phase of the virtual NC-AFM phase shifter is similar to the one of the experimental machine. In the very close vicinity of the surface, as $\varphi(\omega_0) \gtrapprox -\pi/2$, e.g. the amplitude of the oscillations slightly decreases, a weak increase is observed. Curve [b] : As $\varphi(\omega_0)$ varies more quickly than in curve [a] due to the different expression of $H(p)$, a larger increase of the damping is obtained.